

Photodissociation of nitric acid and water in the vacuum ultraviolet; vibrational and rotational distributions of OH $2\Sigma^+$

H. Okabe

Citation: [The Journal of Chemical Physics](#) **72**, 6642 (1980); doi: 10.1063/1.439123

View online: <http://dx.doi.org/10.1063/1.439123>

View Table of Contents: <http://scitation.aip.org/content/aip/journal/jcp/72/12?ver=pdfcov>

Published by the [AIP Publishing](#)

Articles you may be interested in

[Role of OH radicals in the formation of oxygen molecules following vacuum ultraviolet photodissociation of amorphous solid water](#)

J. Chem. Phys. **133**, 104504 (2010); 10.1063/1.3474999

[The vibrationally mediated photodissociation dynamics of nitric acid](#)

J. Chem. Phys. **91**, 2929 (1989); 10.1063/1.456963

[Photodissociation dynamics of water in the second absorption band. I. Rotational state distributions of OH\(\$2\Sigma\$ \) and OH\(\$2\Pi\$ \)](#)

J. Chem. Phys. **87**, 4627 (1987); 10.1063/1.452824

[Initial Rotational Distribution of OH*\(\$2\Sigma^+\$ \) Produced by KrPhotosensitized Decomposition of Water](#)

J. Chem. Phys. **50**, 2775 (1969); 10.1063/1.1671453

[Electronic Quenching and the Rotational Relaxation Rate of OH*\(\$2\Sigma^+\$ \) Produced by the VacuumUltraviolet Photodecomposition of Water](#)

J. Chem. Phys. **48**, 4468 (1968); 10.1063/1.1668016



Photodissociation of nitric acid and water in the vacuum ultraviolet; vibrational and rotational distributions of $\text{OH}^2\Sigma^+$

H. Okabe

Molecular Spectroscopy Division, National Bureau of Standards, Washington, D.C. 20234
(Received 21 December 1979; accepted 26 February 1980)

The absorption cross sections of nitric acid have been measured in the 1100–1900 Å region. The process $\text{HONO}_2 \xrightarrow{h\nu} \text{OH}^2\Sigma + \text{NO}_2$ occurs below 1475 Å, much shorter than the thermochemical threshold at 2040 Å. The $\text{OH}^2\Sigma$ fluorescence yield is less than 2%. The vibrational and rotational distributions of $\text{OH}^2\Sigma$ from HONO_2 photolysis at 1236 Å have been measured and compared with those from H_2O and H_2O_2 photolysis. The excess energy beyond that required to dissociate the molecule and to excite ground state OH to $\text{OH}^2\Sigma$ is converted to rotation and much less to vibration of $\text{OH}^2\Sigma$ in contrast with linear cyanogen molecules where the excess energy appears as vibration and much less as rotation of a CN product. The results of internal energy partitioning have been compared with calculations based on a simple quasidiatomic impulsive model. The deviation from the model is attributed to either a process involving a large change in bond angle or in bond length. The rotational distributions of $\text{OH}^2\Sigma$ at $v' = 0$ show a narrow peak at $N' = 20$ for H_2O photolysis and a broad peak at $N' = 10$ for HONO_2 photolysis both at 1236 Å. The extent of rotational excitation is expressed in terms of an impact parameter. The large impact parameter is found for H_2O and H_2O_2 photolysis while for HONO_2 photolysis the impact parameter is small. The rotational distributions of $\text{OH}^2\Sigma$ from H_2O and H_2O_2 photolysis at 1236 Å deviate completely from Boltzmann behavior while that from HONO_2 approaches the Boltzmann distribution. The process to yield the electronically excited NO_2 from HONO_2 photolysis at 1236 Å is less than 0.5%.

INTRODUCTION

Nitric acid has recently been observed in the stratosphere with a mixing ratio of about 5×10^{-9} at an altitude of 20 km.^{1,2} The photodissociation of nitric acid in the stratosphere may play an important role in determining the atmospheric ozone concentration. In this connection the absorption coefficients of nitric acid in the near ultraviolet have been measured by Johnston and Graham³ and by Biau⁴ and in the vacuum ultraviolet, by Beddard *et al.*⁵ The primary products of photodissociation in the near ultraviolet are found by Johnston *et al.*⁶ to be $\text{OH}(X^2\Pi)$ and NO_2 .

The production of $\text{OH}(A^2\Sigma^+)$ and NO_2 is energetically possible below 2040 Å. This work was initiated to assess the importance of the $\text{OH}(A^2\Sigma^+)$ production in the vacuum ultraviolet photolysis of HONO_2 . The vibrational and rotational distributions of $\text{OH}^2\Sigma^+$ are also obtained from the spectra of the $\text{OH}^2\Sigma^+$ fluorescence produced in the photodissociation of HONO_2 and H_2O by the Kr resonance lamp.

Internal state distributions of photofragments in their ground and excited electronic states have been studied by many workers⁷ with various techniques including time-of-flight distributions of photofragments, absorption spectroscopy, laser induced fluorescence and fluorescence from photofragments. A previous work⁸ on the vibrational and rotational distributions of $\text{CN}(B^2\Sigma)$ formed from the photodissociation of linear triatomic cyanogen molecules is now extended to a study on internal energy distributions of $\text{OH}^2\Sigma$ photodissociated from bent OH-containing molecules, namely, H_2O , H_2O_2 , and HONO_2 . The vibrational and rotational distributions of $\text{OH}^2\Sigma^+$ observed are discussed on the basis of a simple quasidiatomic impulsive model and impact parameters.

Semiclassical and quantum mechanical models have been proposed by various workers in an effort to reproduce the observed results. Most of the recent theories deal with vibrational distributions of a diatomic photofragment dissociated from a linear triatomic molecule and only few^{9,10} consider rotation and bending motion of the parent molecule to provide analytical expressions for rotational distributions of the diatomic product. However, the theory does not cover rotational distributions of the fragment from a bent molecule. It appears that the same theory could be applied to small impact parameter photodissociation of the bent molecule.

EXPERIMENTAL

The absorption cross section of nitric acid was measured as before¹¹ by a combination of a hydrogen lamp and a 1 m near normal incidence vacuum monochromator. Nitric acid at the pressure range 13 to 66 Nm⁻² (0.1 to 0.5 Torr) was introduced into a Monel cell with a path length of 6.95 ± 0.01 cm. The pressure was measured with a calibrated pressure transducer. Because of the occurrence of slow degradation of nitric acid, a fresh sample was introduced into the cell in every 10 min.

The measurements were taken at 2 Å intervals with a scanning speed of 5 Å min⁻¹. The absorption cross section, σ , is defined as $I_t = I_0 l^{-\sigma n}$, where I_t and I_0 are the transmitted and incident light intensities, respectively, n is the number of molecules per cm³ at room temperature, and l is the path length in cm. Undispersed $\text{OH}^2\Sigma$ fluorescence intensities were measured at right angles to the incident monochromatic beam through a broad band filter transmitting light of wavelengths from 2200 to 4200 Å. The scanning speed was 5 Å min⁻¹ with a time constant of 5 sec. The fluorescence efficiency

curve was constructed by plotting the fluorescence intensity normalized to that of incident light as a function of incident wavelength with a slit width of 200 μm corresponding to a nominal resolution of 3 \AA . In another series of experiments the $\text{OH}(^2\Sigma^+)$ fluorescence was produced by irradiating low pressure (0.1 to 0.2 Torr) flowing samples with the Kr (1165, 1236 \AA) resonance lamp. The fluorescence spectra were taken in the second order by means of a 0.3 m plane grating monochromator with a 1200 grooves mm^{-1} grating (blaze wavelength 5000 \AA) at a slit width of 80 μm corresponding to a nominal resolution of 1 \AA . The scanning speed was 10 $\text{\AA}/\text{min}^{-1}$. Anhydrous nitric acid was prepared by vacuum distillation from concentrated sulfuric acid and sodium nitrate³ and was kept at liquid nitrogen temperature.

RESULTS

Absorption

Figure 1 shows the absorption cross sections of nitric acid in the region from 1100 to 1900 \AA . The 1300 to 1800 \AA region was measured at a slit width of 50 μm corresponding to a nominal resolution of 1 \AA , 1100 to 1300 \AA , at a resolution of 2 \AA and 1800 to 1900 \AA , at a resolution of 3 \AA . The estimated error in the 1800 to 1900 \AA region is within 10% and in the region below 1800 \AA , within 5%. The values at 1900 and 1850 \AA are about 20% to 30% lower than those by Johnston and Graham³ and by Biaume,⁴ while in the 1450 to 1700 \AA region values are in reasonable agreement with those by Beddard *et al.*⁵ obtained with a resolution of 15 \AA . Higher absorption cross sections obtained by Beddard *et al.* below 1300 \AA may be ascribed to the presence of NO_2 impurities in their sample. No peaks have been found at 1640 and 1460 \AA predicted by Harris.¹² The absorption spectrum may be divided into several regions with absorption peaks at 1820, 1360, 1290, 1215, 1155, and 1105 \AA . The 1820 \AA absorption is very broad and very diffuse, followed by an absorption with the highest peak ($\sigma = 26.5 \times 10^{-18} \text{ cm}^2$) at 1360 \AA . Several diffuse

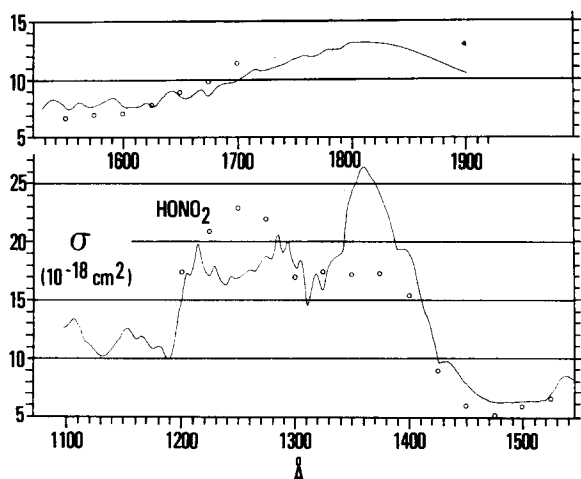


FIG. 1. Absorption cross section σ of nitric acid in the 1100 to 1900 \AA region; pressure, 0.1 to 0.5 Torr; resolution, 3 \AA (1800 to 1900 \AA), 1 \AA (1300 to 1800 \AA) 2 \AA (1100 to 1300 \AA). (Δ) from Ref. 3; (\bullet) from Ref. 4; (\circ) from Ref. 5.

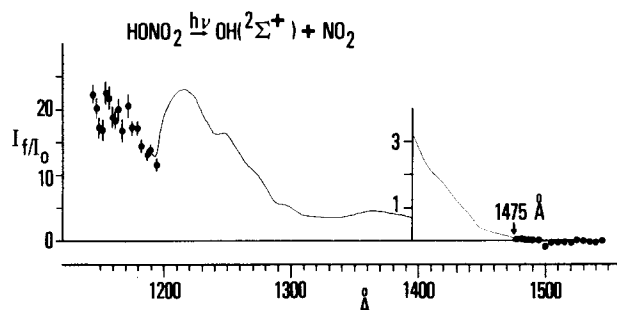


FIG. 2. Fluorescence efficiency curve of $\text{OH}(^2\Sigma^+)$ from 0.2 Torr nitric acid in arbitrary units; fluorescence intensities normalized to incident intensities; resolution, 3 \AA ; the absolute yield at 1236 \AA is 0.02.

bands in the 1500 to 1700 \AA region may represent a vibrational progression. Towards shorter wavelengths the absorption spectrum shows many less diffuse bands which may correspond to Rydberg transitions.

Fluorescence

Figure 2 shows the $\text{OH}(^2\Sigma)$ fluorescence curve I_f/I_0 as a function of incident wavelength, where I_f is the fluorescence intensity and I_0 is the incident intensity. The fluorescence appears only below $1475 \pm 2 \text{ \AA}$, and the yield is still very low in the 1360 \AA region of absorption. It starts to increase below 1300 \AA and the absolute yield at 1236 \AA is about 0.02 in comparison with that of 0.05 for water.¹³

VIBRATIONAL AND ROTATIONAL DISTRIBUTION OF $\text{OH}(^2\Sigma^+)$

Both the (1, 0) and (0, 0) bands of $\text{OH}(^2\Sigma^+)$ are formed in the photodissociation of H_2O and HONO_2 by the Kr (1236, 1165 \AA) lamp. The fluorescence intensity ratios at 1236 and 1165 \AA can be estimated from the line intensity ratio of about 4 of the lamp¹⁴ and the ratios of absorption coefficient of about 3 and 1.4 at these wavelengths for H_2O (Ref. 15) and HONO_2 , respectively. The fluorescence intensity ratios thus obtained are 12 and 6 for H_2O and HONO_2 , respectively; that is, the $\text{OH}(^2\Sigma^+)$ fluorescence arises predominantly from the 1236 \AA excitation. Figure 3 gives the low resolution (3 \AA) spectra of $\text{OH}(^2\Sigma^+)$ fluorescence produced from irradiating 0.06 Torr water by the Kr lamp. The integrated (1, 0) to (0, 0) intensity ratio is 0.1 when corrected for grating efficiency. Figure 4 shows the $\text{OH}(^2\Sigma^+)$ fluorescence spectrum obtained from the photodissociation of 0.13 Torr nitric acid by the Kr lamp. The (1, 0) to (0, 0) ratio is 0.1. The fluorescence spectra of the $\text{OH}(^2\Sigma - ^2\Pi)$ (0, 0) band are shown in Figs. 5 and 6 at a resolution of 1 \AA when water and nitric acid at 0.2 Torr, respectively, are irradiated by the Kr lamp. Welge *et al.*¹⁶ found no change in the rotational distribution within the pressure range 0.05 to 1 Torr of H_2O indicating that rotational relaxation is much slower than electronic quenching by H_2O . No apparent change of rotational distribution is observed in the 0.1 to 0.2 Torr region of HONO_2 . The rotational assignments follow those by Dieke and Crosswhite.¹⁷ The vibrational population is obtained from the observed emission intensity, $I_{\nu', \nu''}$, divided by

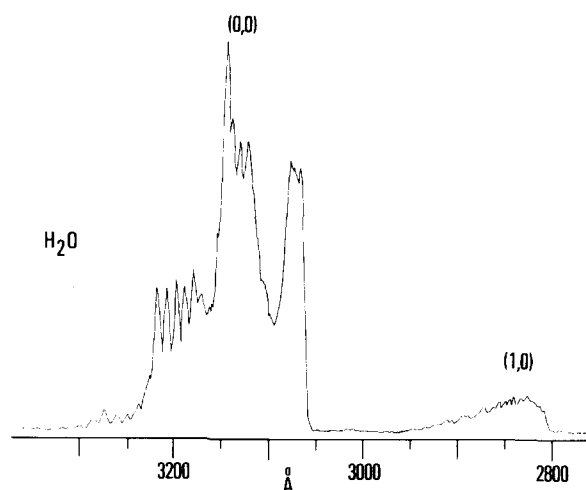


FIG. 3. Low resolution (3 Å) fluorescence spectrum of $\text{OH}(^2\Sigma^+)$ from the photolysis of 0.06 Torr H_2O by the Kr lamp; the (1,0) to (0,0) band intensity ratio is about 0.1.

$A_{\nu',\nu''}$, where $A_{\nu',\nu''}$ is the Einstein transition probability and ν',ν'' is the wave number for the ν' to ν'' transition. Since the ratio, $A_{0,0\nu_{0,0}/A_{1,0\nu_{1,0}}}$, is 2.75,¹⁸ the population at $\nu'=1$ to that at $\nu'=0$ is 0.28 for $\text{OH}(^2\Sigma)$ photodissociated from H_2O and HONO_2 at 1236 Å. On the other hand, the corresponding population for $\text{OH}(^2\Sigma)$ from H_2O_2 at 1236 Å is less than 0.02.¹⁹ These results are presented in Table I. The rotational populations at various N' (the rotational quantum number of the upper state) can be found from the observed intensities divided by the calculated transition probabilities by Learner.²⁰

The rotational distributions of $\text{OH}(^2\Sigma)$ in $\nu'=0$ thus obtained are given in Table II for H_2O , H_2O_2 , and HONO_2 photodissociation, and are shown in Figs. 7 and 8 for H_2O and HONO_2 , respectively. Because the rotational levels above $N'=23$ predissociate,²¹ populations given in Table II are corrected accordingly for these levels. The rotational distributions of $\text{OH}(^2\Sigma^*)$ from H_2O show a sharp maximum at $N'=20$, while in HONO_2 the peak is

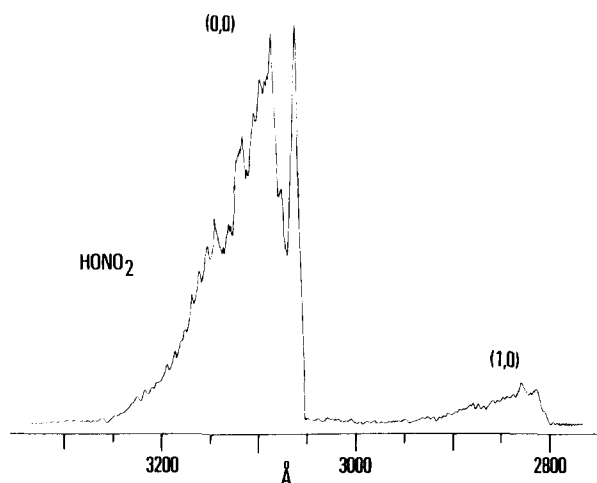


FIG. 4. Low resolution (3 Å) fluorescence spectrum of $\text{OH}(^2\Sigma^+)$ from the photolysis of 0.13 Torr HONO_2 by the Kr lamp; the (1,0) to (0,0) band intensity ratio is about 0.1.

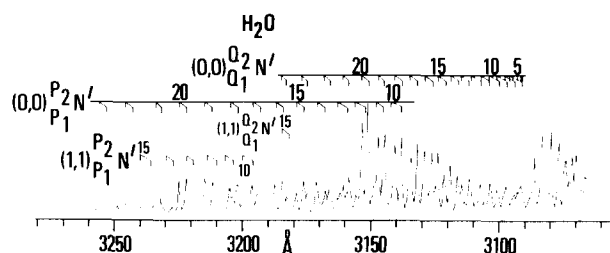


FIG. 5. Fluorescence spectrum of the $\text{OH}(^2\Sigma^+ \rightarrow ^2\Pi)$ (0,0) band in the photodissociation of 0.2 Torr H_2O by the Kr lamp (mainly 1236 Å); resolution, 1 Å. The rotational quantum numbers N' are those of the upper state.

broader and shifts to $N'=10$. The rotational distribution of $\text{OH}(^2\Sigma^*)$ from H_2O is very similar to that obtained by Carrington originally¹³ and more recently by Vikis.²²

EMISSION FROM ELECTRONICALLY EXCITED NO_2

An attempt was made to detect the production of an electronically excited $\text{NO}_2(\text{NO}_2^*)$ in the photodissociation of HONO_2 by the Kr lamp. The emission from NO_2^* produced by $\text{O} + \text{NO}$ chemiluminescence or by light absorption above 4000 Å lies in the 4000 to 14 000 Å region with a maximum at 6500 Å.²³ With a 500 μm slit width corresponding to a band width of 16 Å, the photolysis of 0.12 Torr NONO_2 by the Kr lamp gave 60 divisions at the peak of $\text{OH}(^2\Sigma \rightarrow ^2\Pi)$ (1,0) band in the second order, while the signal in the 4600 to 6000 Å region was less than one division with a photomultiplier of S-13 spectral response. From the data the absolute yield of NO_2^* is estimated to be less than 0.5%.

DISCUSSION

Fluorescence excitation spectrum

The thermochemical threshold energy for the process $\text{HONO}_2 \rightarrow \text{OH} + \text{NO}_2$ is $199 \pm 1.7 \text{ kJ mol}^{-1}$ which can be calculated from the heats of formation (in kJ mol^{-1}), -124 ± 0.4 , 38.9 ± 1.3 , and 35.9 ± 0.8 at 0°K for HONO_2 , OH , and NO_2 respectively.²⁴ Since the electronic energy¹⁷ of $\text{OH}(^2\Sigma^*)$ is 388 kJ mol^{-1} , the corresponding process to form $\text{OH}(^2\Sigma^*)$ requires $587 \pm 1.7 \text{ kJ mol}^{-1}$ which corresponds to the incident wavelength $2040 \pm 7 \text{ Å}$. However, the $\text{OH}(^2\Sigma^*)$ production is apparent only below 1475 Å indicating that absorption of light in the 1820 Å region yields ground state OH and NO_2 . Similar observation was made by Becker *et al.*¹⁹ in the photolysis of H_2O_2

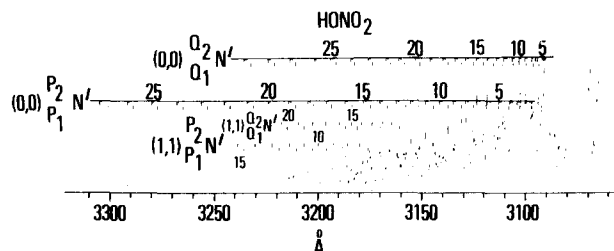


FIG. 6. Fluorescence spectrum of the $\text{OH}(^2\Sigma^+ \rightarrow ^2\Pi)$ (0,0) band in the photodissociation of 0.2 Torr HONO_2 by the Kr lamp (mainly 1236 Å); resolution, 1 Å. The rotational quantum numbers refer to the upper state.

TABLE I. Vibrational populations of $\text{OH}(\Sigma^+)$ in the photodissociation of H_2O , H_2O_2 , and HONO_2 .

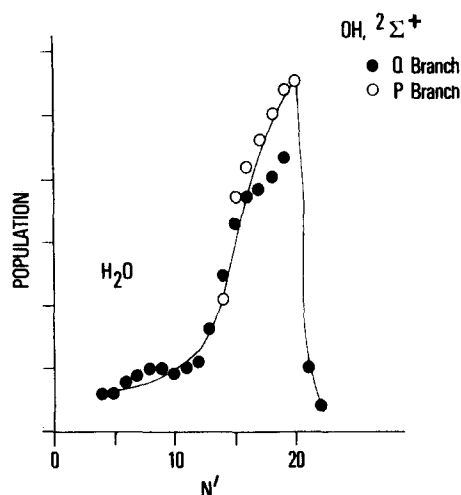
| Vibrational level ^a | cm^{-1} | Population | | | |
|--------------------------------|------------------|-------------------------|---------------------|--|---------------------------------|
| | | H_2O at | | H_2O_2 ^d at | HONO_2 ^c at |
| v' | | 1216 Å ^b | 1236 Å ^c | 1236 Å | 1236 Å |
| 0 | 0 | 1 | 1 | 1 | 1 |
| 1 | 2989 | 0.3 | 0.28 | <0.02 | 0.28 |
| 2 | 5782 | <0.01 | | | |

^aFrom Ref. 17.^cThis work.^bFrom Ref. 13.^dFrom Ref. 19.

that $\text{OH}(\Sigma^+)$ is not produced even at 1849 Å, while the thermochemical threshold is at 2010 Å. On the other hand the $\text{OH}(\Sigma^+)$ production from H_2O is observed below 1360 Å (Ref. 25) in excellent agreement with the thermochemical threshold at 1356 ± 3 Å. The results indicate that the $\text{OH}(\Sigma^+)$ production process in H_2O_2 and HONO_2 must involve a high potential energy barrier. The $\text{OH}(\Sigma^+)$ fluorescence efficiency curve of Fig. 2 shows almost no structure in comparison with the absorption spectrum of Fig. 1, indicating that the $\text{OH}(\Sigma^+)$ state originates from direct dissociation of the molecule on a repulsive surface.

TABLE II. Rotational populations of $\text{OH}(\Sigma^+)$, $v' = 0$ in the photodissociation of H_2O , H_2O_2 , and HONO_2 .

| Rotational level ^a | | Population (total = 1.00) ^b | | | |
|-------------------------------|------------------|--|---------------------|--|---------------------------------|
| | | H_2O at | | H_2O_2 ^e at | HONO_2 ^d at |
| N' | cm^{-1} | 1216 Å ^c | 1236 Å ^d | 1236 Å | 1236 Å |
| 1 | 34 | ... | ... | ... | 0.03 |
| 2 | 102 | 0.009 | ... | 0.01 | 0.04 |
| 3 | 203 | 0.009 | ... | 0.01 | 0.04 |
| 4 | 338 | 0.009 | 0.016 | 0.02 | 0.04 |
| 5 | 507 | 0.009 | 0.016 | 0.02 | 0.05 |
| 6 | 709 | 0.009 | 0.019 | 0.02 | 0.05 |
| 7 | 944 | 0.009 | 0.023 | 0.02 | 0.06 |
| 8 | 1211 | 0.009 | 0.023 | 0.02 | 0.06 |
| 9 | 1511 | 0.009 | 0.026 | 0.02 | 0.07 |
| 10 | 1842 | 0.012 | 0.029 | 0.021 | 0.06 |
| 11 | 2205 | 0.012 | 0.029 | 0.023 | 0.06 |
| 12 | 2592 | 0.03 | 0.039 | 0.025 | 0.05 |
| 13 | 3021 | 0.03 | 0.046 | 0.03 | 0.04 |
| 14 | 3473 | 0.036 | 0.065 | 0.04 | 0.03 |
| 15 | 3955 | 0.045 | 0.082 | 0.045 | 0.03 |
| 16 | 4465 | 0.06 | 0.092 | 0.050 | 0.03 |
| 17 | 5002 | 0.069 | 0.10 | 0.053 | 0.02 |
| 18 | 5566 | 0.081 | 0.11 | 0.055 | 0.02 |
| 19 | 6156 | 0.12 | 0.12 | 0.06 | 0.02 |
| 20 | 6771 | 0.135 | 0.13 | 0.065 | 0.02 |
| 21 | 7410 | 0.144 | 0.03 | 0.06 | 0.01 |
| 22 | 8072 | 0.15 | | 0.06 | 0.01 |
| 23 | 8757 | 0.024 | | 0.05 | 0.01 |
| 24 | 9462 | | | (0.049) 0.05 | (0.008) 0.01 |
| 25 | 10188 | | | (0.036) 0.045 | (0.006) 0.009 |
| 26 | 10933 | | | (0.26) 0.040 | (0.005) 0.01 |
| 27 | 11696 | | | (0.016) 0.05 | |
| 28 | 12476 | | | (0.007) 0.04 | |

^aFrom Ref. 17.^dThis work.^bCorrected for prodissociation for $N' > 23$.^eFrom Ref. 19.^cFrom Ref. 13.FIG. 7. Rotational population distribution of $\text{OH}(\Sigma^+)$, $v' = 0$ state in the photodissociation of 0.2 Torr H_2O by the Kr lamp (mainly 1236 Å) (●) Q branch; (○) P branch; N' is the rotational quantum number of the upper state.

Energy partitioning in photodissociation

Conceptually, photodissociation may be divided into two steps, that is, a fast initial step of light absorption from the ground to an electronically excited state fol-

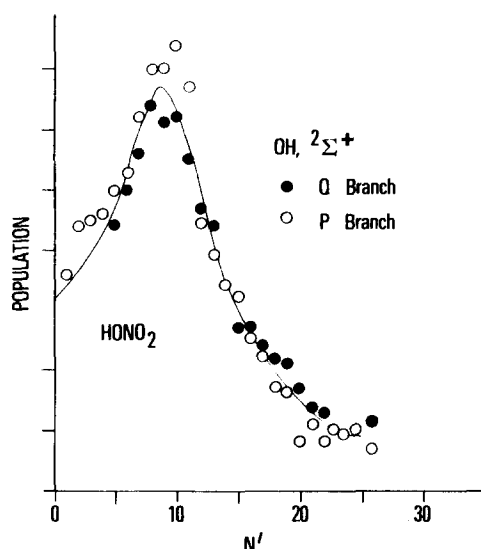


FIG. 8. Rotational population distribution of $\text{OH}(^2\Sigma^+)$, $v' = 0$ state in the photodissociation of 0.2 Torr H_2O by the Kr lamp (mainly 1236 Å) (●) Q branch; (○) P branch; N' is the rotational quantum number of the upper state.

lowed by a slow dissociating step on a repulsive surface into fragments. The transition probability of the first step is governed by the Franck-Condon factors involving the vibrational wavefunctions of the ground and upper states. Suppose the molecule is formed in the upper state with the equilibrium bond length different from those of the ground state and a diatomic photofragment vibration of the diatomic fragment may be excited in the dissociation process. The change in bond angle in the upper state provides a necessary torque to excite rotation as the fragments dissociate on a repulsive surface. On the other hand if the equilibrium conformation remains the same during light absorption, vibration of the diatomic fragment may be excited by a repulsive force acting along the internuclear axis and rotation may be excited by a torque produced by bending vibration of the parent molecule as the fragments separate on the repulsive surface.

To explain energy partitioning in photodissociation of a triatomic molecule Holdy *et al.*²⁶ and Busch and Wilson²⁷ proposed a simple classical quasidiatomic model in which the molecule ABC is considered as diatomic A-(BC) and photon absorption only affects the breaking bond A-B. That is, the molecule is formed on a repulsive surface and the dissociation is immediate without change in the B-C bond distance and the A-B-C bond angle. The available energy E_{avl} , the energy left over after bond scission and any electronic excitation of fragments, is initially converted into the translational energy of the two atoms A and B in a dissociation process



The kinetic energy in B is subsequently transformed into the vibrational, rotational and translational energies of BC. From the conservation of linear and angular momentum between A and B and A and BC, respectively, the following relation are derived:

$$E_{\text{int}}/E_{\text{avl}} = 1 - \mu_a/\mu_f, \quad (1)$$

$$E_v/E_{\text{avl}} = (1 - \mu_a/\mu_f) \cos^2 \chi, \quad (2)$$

$$E_r/E_{\text{avl}} = (1 - \mu_a/\mu_f) \sin^2 \chi, \quad (3)$$

where E_{avl} is the available energy beyond that required to dissociate the molecule and excite the fragments electronically, E_{int} is the sum of vibrational and rotational energies of the fragment BC, and E_v and E_r are vibrational and rotational energies, respectively. The reduced mass of the two atoms A and B and that of A and BC are μ_a and μ_f , respectively, and χ is the bond angle at the time of dissociation.

Morse, Freed, and Band^{9,10} have recently developed a quantum theory of photodissociation of a linear triatomic molecule using the correct normal modes of the initial state of the molecule. To express the rotational angular momentum distributions of the diatomic product, the rotational and bending degrees of freedom of the parent molecule are included. The important conclusion of this theory is that when the deviation of the molecule from linearity is small, the distribution of diatomic rotational angular momentum J follows that of the parent molecule J , because of the imposition of the conservation of angular momentum. It is also assumed that the interaction of the fragment vibration and rotation with the relative translational motion of the fragments may be neglected during the period of the final separation. However, the theory has not been extended to include the rotational distribution of a bent molecule or to cases where a large change in bond angle is involved.

The results of the present work are discussed on the basis of the preceding qualitative quasidiatomic impulsive model and theory of collinear dissociation of triatomic molecules. Without further information on the structure of the excited states and the shape of the repulsive potential surfaces involved, more sophisticated quantitative treatment of energy disposal may not be justified.

Energy partitioning in bent and linear molecules

The fraction of the available energy E_{avl} going into vibration and rotation has been calculated and is presented in Table III for the photodissociation of OH-containing (bent) and CN-containing (linear) molecules. The available energy E_{avl} is given by $E_{\text{avl}} = h\nu - D_0 - E_0$, where $h\nu$ is the incident photon energy, D_0 is the dissociation energy of the breaking bond, and E_0 is the electronic energy of the fragment. The following bond dissociation energies²⁴ and the electronic energies are used to calculate E_{avl} in Table III; $D_0(\text{H}-\text{OH}) = 41\,280 \pm 100 \text{ cm}^{-1}$, $D_0(\text{HO}-\text{OH}) = 17\,400 \pm 140 \text{ cm}^{-1}$, $D_0(\text{HO}-\text{HO}_2) = 16\,700 \pm 140 \text{ cm}^{-1}$, $E_0(\text{OH}, ^2\Sigma)$ (Ref. 17) = $32\,440 \text{ cm}^{-1}$, $E_0(\text{CN}, B^2\Sigma)$ (Ref. 28) = $25\,800 \text{ cm}^{-1}$, $E_0(\text{CN}, A^2\Pi)$ (Ref. 28) = $9\,118 \text{ cm}^{-1}$. The bond dissociation energies for cyanogen compounds are taken from Ref. 29 (Table VI). The fractions of E_{avl} going into vibration and rotation for H_2O , H_2O_2 , and HONO_2 photodissociation are calculated using the data of Tables I and II. It is clear from Table III that the fraction of E_{avl} converted to rotation of $\text{OH}(^2\Sigma)$ is much greater than that converted to vibration for bent molecules H_2O , H_2O_2 , and HONO_2 . The results can be explained from Eqs. (2) and (3) that if dissociation

TABLE III. Distribution of excess energy in photodissociation.

| Molecule | λ_{exc} (Å) | E_{avl}^a (cm ⁻¹) | Process ^b | Ground state bond angle | Conversion of excess energy into diatomic fragments | | Ref. |
|-------------------------------|-------------------------------|---|-------------------------|----------------------------------|--|----------|--------------------|
| | | | | | vibration | rotation | |
| (a) Bent molecules | | | | | | | |
| H ₂ O | 1236 | 7 200 | H+OH (A) | H—O—H angle ^c | 0.10 | 0.61 | This work |
| | 1216 | 8 540 | | 105° | 0.08 | 0.68 | 13 |
| H ₂ O ₂ | 1236 | 31 100 | OH+OH (A) | H—O—O angle ^d 98° | < 0.002 | 0.23 | 19 |
| HONO ₂ | 1236 | 31 800 | NO ₂ +OH (A) | H—O—N angle ^e 103° | 0.02 | 0.07 | This work |
| (b) Linear molecules | | | | | | | |
| HCN | 1236 | 14 000 | H+CN (B) | 180° ^f | 0.12 | 0.07 | g |
| | 1216 | 15 300 | H+CN (B) | | 0.12 | 0.06 | h |
| ClCN | 1236 | 21 200 | Cl+CN (B) | 180° ^f | 0.28 | 0.21 | g |
| | 1470 | 8 300 | Cl+CN (B) | j | 0.08 | 0.12 | 32 |
| | 1700 | 25 000 | Cl+CN (X) | j | 0.05 | 0.05 | calc. from Ref. 33 |
| BrCN | 1236 | 26 100 | Br+CN (B) | 180° ^f | 0.21 | 0.07 | g |
| | 1216 | 27 400 | Br+CN (B) | | 0.15 | 0.05 | i |
| ICN | 1236 | 29 600 | I+CN (B) | 180° ^f | 0.23 | 0.10 | g |
| C ₂ N ₂ | 1600 | 8 600 | CN+CN (A) | linear ^c | 0.18 | 0.11 | 38 |

^a $E_{\text{avl}} = h\nu - D_0 - E_0$, see text.^bUnspecified products are those formed in the ground state.^cFrom G. Herzberg, *Molecular Spectra and Molecular Structure. III. Electronic Spectra and Electronic Structure of Polyatomic Molecules* (Van. Nostrand, Princeton, N. J., 1966).^dFrom P. A. Giguere and T. K. K. Srinivasan, *J. Mol. Spectrosc.* **66**, 168 (1977).^eFrom Ref. 41.^fFrom Ref. 24.^gFrom Ref. 8.^hFrom S. Tatematsu and K. Kuchitsu, *Bull. Chem. Soc. Jpn.* **50**, 2896 (1977).ⁱFrom S. Tatematsu, T. Kondow, T. Nakagawa, and K. Kuchitsu, *Bull. Chem. Soc. Jpn.* **50**, 1056 (1977).^jThe upper state may be bent to give more rotation than expected from linear conformation. See text.

occurs near a bond angle of 100°, rotational excitation is much more favored than vibrational excitation. The fractions of E_{avl} released to vibration are much less than those expected from equipartitioning of all vibrational degrees of freedom, indicating that the dissociation is immediate for the three molecules. The absorption spectra of H₂O,³⁰ H₂O₂,³¹ and HONO₂ are very diffuse at 1236 Å suggesting direct dissociation.

On the other hand vibrational excitation of CN($B^2\Sigma$) (and CN, $X^2\Sigma$ for C₂N₂) must be more favorable than rotational excitation for the linear triatomic cyanogen molecules, if dissociation take place near an angle of 180°, which is supported by the results. This simple interpretation does not always hold at other wavelengths where a bent excited state may be involved. Such are the cases for the photolysis of ClCN at 1470 Å (Ref. 32) and near 1700 Å,³³ where the fraction of E_{avl} converted to rotation is greater than or equal to that to vibration.

The fractions of E_{avl} partitioned into internal energies of fragments are calculated for several simple molecules from Eq. (1) and are shown in Table IV. Large discrepancies between the calculated and observed values for H₂O and H₂O₂ at 1236 Å indicate the breakdown of the assumption that there is little change in bond angle

during photodissociation, while the photolysis of H₂O at 1600 Å must occur without change in configuration, because of the agreement between the calculated and observed results. According to the results of recent calculation of the potential energy surface of the A(1B_1) (Ref. 34) and B(1A_1) (Ref. 35) states of H₂O, which correlate with H+OH($^2\Pi$) and H+OH($^2\Sigma$), respectively, the A(1B_1) state dissociates directly into the products without change in configuration, while the B(1A_1) state is linear in its equilibrium conformation.

The internal energy [mostly in vibration of CN($B^2\Sigma$)] found for HCN photolysis at 1216 Å is much larger than that expected from the impulsive model, suggesting that the CN bond length in the excited state may be very different from that in the ground state, the assumption neglected in the impulsive model. Much smaller fraction of E_{int} than that expected from the model is found for the photolysis of ClCN near 1700 Å. The results may be understood on the basis of another model proposed by Holdy *et al.*²⁶ for the photolysis of ICN, where they assume a repulsive force formed between the breaking I-C bond acting on the harmonic oscillator CN. The calculated results show that only a small fraction of E_{avl} is partitioned into the internal energy of CN.

TABLE IV. Internal energy partitioning by a quasidiatomic impulsive model.

| Molecule | λ_{exc} (Å) | E_{avl} (cm ⁻¹) | Process ^a | $E_{\text{int}}/E_{\text{avl}}$ | | Ref. |
|-------------------------------|-------------------------------|---|----------------------|---------------------------------|-------------------|-----------|
| | | | | Calc. | Obs. | |
| H ₂ O | 1236 | 7 180 | H+OH (A) | 0.003 | 0.71 | This work |
| | 1600 | 21 100 | H+OH | 0.003 | 0.01 | 39 |
| H ₂ O ₂ | 1236 | 31 140 | OH+OH (A) | 0.06 | 0.36 ^f | 19 |
| HCN | 1216 | 15 300 | H+CN (B) | 0.04 | 0.18 | b |
| ClCN | 1236 | 21 200 | Cl+CN (B) | 0.40 | 0.49 | c |
| | 1700 | 25 000 | Cl+CN | 0.40 | 0.10 | 33 |
| BrCN | 1236 | 26 100 | Br+CN (B) | 0.47 | 0.28 | c |
| ICN | 1236 | 29 600 | I+CN (B) | 0.49 | 0.33 | c |
| ClNO | 3471 | 16 000 | Cl+NO | 0.38 | 0.30 | d |
| NO ₂ | 3471 | 4 130 | O+NO | 0.28 | 0.40 | e |

^aUnspecified photofragments are those formed in the ground state.

^bFrom S. Tatematsu and K. Kuchitsu, *Bull. Chem. Soc. Jpn.* **50**, 2896 (1967).

^cFrom Ref. 8.

^dFrom G. E. Busch and K. R. Wilson, *J. Chem. Phys.* **56**, 3655 (1972).

^eFrom Ref. 27.

^fBoth OH radicals are assumed to have the same rotational energy.

Rotational distribution in photodissociation

If we assume that upon light absorption a molecule dissociates into two fragments R_1 and R_2 , with masses m_1 and m_2 , the degree of rotational angular momentum of the fragments may be expressed by the impact parameter b , defined by the perpendicular distance from the center of mass of the fragment R_1 to a line extrapolated back from the distant straight line trajectory of the fragment R_2 .¹³

A large impact parameter signifies a long range interaction of noncentral character between the two departing photofragments involving a large change in bond angle. A large rotational angular momentum of R_1 is accompanied by an equally large rotational angular momentum of R_2 in opposite direction, if the contribution from the angular momentum of the parent molecule is neglected. Then the impact parameter is given by

$$b = [1/(2\mu E_{\text{tr}})^{1/2}](\hbar/2\pi)[N(N+1)]^{1/2} \quad (4)$$

where $\mu = m_1 m_2 / m_1 + m_2$, N is the rotational angular momentum of the fragment, and E_{tr} is the translational energy of both fragments. Table V shows that both H₂O and H₂O₂ dissociate into the respective products with a large change in bond angle, while HONO₂ and ICN dissociate into the products with only a small change in bond angle and a small bending vibration would be sufficient to excite the observed rotation of diatomic fragments.

In a series of papers Morse, Freed, and Band^{9,10} have proposed the general quantum theory of collinear photodissociation of triatomic molecules. By including hitherto neglected rotational and bending degrees of freedom of the parent molecule, the theory provides analytical expressions for rotational angular momentum distributions of the products. Under the assumption that the product state distribution is governed by the Franck-Condon factor alone, the theory concludes that because of the conservation of angular momentum the product rotational distributions follow those of the

TABLE V. Impact parameters in photodissociation.

| Molecule | E_{exc} (Å) | E_{tr} (cm ⁻¹) | Process ^a | Impact parameter (Å) | Change of angle (deg) | Ref. |
|-------------------------------|-------------------------|--|-------------------------|----------------------------|--------------------------------|-----------|
| H ₂ O | 1236 | 640 ^b | H+OH (A) | 3.42 | 75 | This work |
| | 1216 | 680 ^b | | 3.6 | | 13 |
| H ₂ O ₂ | 1236 | 17 600 ^c | OH+OH (A) | 0.22 | 20 | 19 |
| HONO ₂ | 1236 | 28 100 ^d | NO ₂ +OH (A) | 0.07 | ~3 | This work |
| ICN | 1236 | 26 400 | I+CN (B) | 0.22 | 5 | e |

^aUnspecified fragments are those formed in the ground state.

^b200 cm⁻¹ thermal energy is assumed for H₂O.

^cOH is assumed to have the same rotational energy as OH(A).

^dNO₂ is assumed to have the same rotational energy as OH(A).

^eFrom Ref. 8.

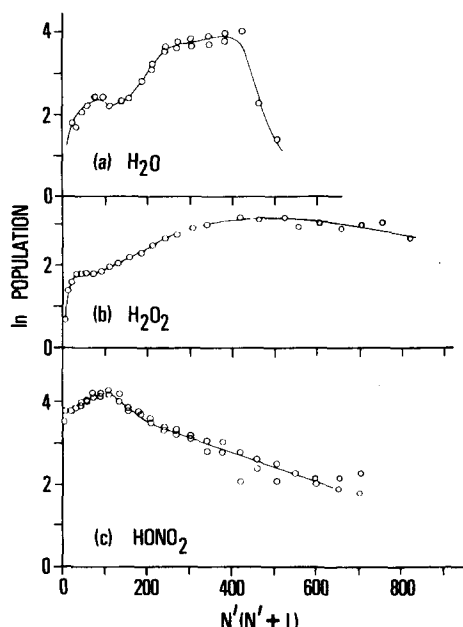


FIG. 9. Plots of \ln rotational population of $\text{OH}(^2\Sigma)$, $v' = 0$ against $N'(N' + 1)$. (a) $\text{OH}(^2\Sigma)$ from the photolysis of H_2O at 1236 Å. (b) $\text{OH}(^2\Sigma)$ from the photolysis of H_2O_2 at 1236 Å; predissociation for $N' > 23$ is corrected; data taken from Ref. 19. (c) $\text{OH}(^2\Sigma)$ from the photolysis of HONO_2 at 1236 Å; predissociation for $N' > 23$ is corrected.

parent molecule for small impact parameter dissociation, that is, the product rotational distribution approximates the Boltzmann distribution of the parent molecule at room temperature. This Boltzmann behavior has been observed for $\text{CN}(B)$ from HCN photolysis³⁶ at 1470 Å, BrCN (Ref. 37) at 1580 Å, and for $\text{CN}(X)$ from C_2N_2 (Ref. 38) near 1600 Å, all linear molecules in the ground state. The Boltzmann distribution is also found for $\text{OH}(X^2\Pi)$ from 1600 Å photolysis of H_2O ,³⁹ where ground state OH has a maximum at $N'' = 2$, while H_2O has a maximum at $J'' = 3$ at room temperature. To a first approximation it can be assumed that the axis of rotation in H_2O is the c axis, perpendicular to the molecular plane, at room temperature, since the rotational constant about the c axis is the smallest. As the H atom separates from H_2O on the molecular plane during molecular rotation, the c axis becomes the axis of rotation of OH radical. Because the rotational constant of H_2O (9.285 cm^{-1}) is much smaller than that of $\text{OH}(X^2\Pi)$ (18.515 cm^{-1}), E_{rot} is partially dissipated to provide required rotational energy of OH by bending vibration. In HONO_2 photodissociation, the axis of rotation is also the c axis perpendicular to the molecular plane and the c axis becomes the axis of rotation of $\text{OH}(^2\Sigma)$ as NO_2 moves away from $\text{OH}(^2\Sigma)$. The dissociation process is similar to that of a linear triatomic molecule in which the axis of rotation of the molecule coincides with that of the dissociating diatomic fragment. Hence it is expected that the rotational distribution of $\text{OH}(^2\Sigma)$ exhibits Boltzmann character in the photodissociation of HONO_2 , although calculation of the rotational distribution of the fragment has not been extended to the photodissociation of bent molecules.¹⁰

To see whether the rotational distribution follows

Boltzmann character, $\ln\text{OH}(^2\Sigma)$ rotational population is plotted against $N'(N' + 1)$ for H_2O , H_2O_2 , and HONO_2 photodissociation at 1236 Å, which is shown in Fig. 9 using the data from Table II. A correction has been made for predissociation of $\text{OH}(^2\Sigma)$, $v' = 0$ above $N' = 24$. As expected the $\text{OH}(^2\Sigma)$ rotational distributions for H_2O and H_2O_2 photodissociation deviate entirely from the Boltzmann plot, while for HONO_2 photodissociation, the distribution approximates that of Boltzmann except for $N' < 10$ with a rotational temperature of 6600 °K. The conservation of angular momentum requires $J = j_1 + j_2$ (Ref. 40) for dissociation of polyatomic molecules, where J is the rotational angular momentum of the parent molecule and j_1 , j_2 are those of the fragments. The maximum J at room temperature is 22 using a rotational constant of 0.2088 cm^{-1} .⁴¹ Since $j_1(\text{OH } ^2\Sigma) = 10$, $j_2(\text{NO}_2)$ becomes 12, indicating that the two fragments are formed with almost equal rotational distribution.

- ¹W. J. Williams, J. N. Brooks, D. G. Murcray, and F. H. Murcray, *J. Atmos. Sci.* **29**, 1375 (1972).
- ²M. Loewenstein and W. L. Starr, *Geophys. Res. Lett.* **5**, 531 (1978).
- ³H. Johnston and R. Graham, *J. Phys. Chem.* **77**, 62 (1973).
- ⁴F. Biau, *J. Photochem.* **2**, 139 (1973–1974).
- ⁵G. S. Beddard, D. J. Giachardi, and R. P. Wayne, *J. Photochem.* **3**, 321 (1974–75).
- ⁶H. S. Johnston, S. G. Chang, and C. Whitten, *J. Phys. Chem.* **78**, 1 (1974).
- ⁷J. P. Simons, *Chemical Society Specialist Periodical Reports, Gas Kinet. Energy Transfer* **2**, 53 (1977); H. Okabe, *Photochemistry of Small Molecules* (Wiley-Interscience, New York, 1978), pp. 81.
- ⁸A. Mele and H. Okabe, *J. Chem. Phys.* **51**, 4798 (1969).
- ⁹M. D. Morse, K. F. Freed, and Y. B. Band, *Chem. Phys. Lett.* **44**, 125 (1976).
- ¹⁰M. D. Morse, K. F. Freed, and Y. B. Band, *J. Chem. Phys.* **70**, 3604 (1979); **70**, 3620 (1979).
- ¹¹H. Okabe and V. H. Dibeler, *J. Chem. Phys.* **59**, 2430 (1973).
- ¹²L. E. Harris, *J. Chem. Phys.* **58**, 5615 (1973).
- ¹³T. Carrington, *J. Chem. Phys.* **41**, 2012 (1964).
- ¹⁴H. Okabe, *J. Opt. Soc. Am.* **54**, 478 (1964).
- ¹⁵K. Watanabe and M. Zelickoff, *J. Opt. Soc. Am.* **43**, 753 (1953).
- ¹⁶K. H. Welge, S. V. Filseth, and J. Davenport, *J. Chem. Phys.* **53**, 502 (1970).
- ¹⁷G. H. Dieke and H. M. Crosswhite, *J. Quant. Spectrosc. Radiat. Transfer* **2**, 97 (1962).
- ¹⁸D. R. Crosley and R. K. Lengel, *J. Quant. Spectrosc. Radiat. Transfer* **15**, 579 (1975).
- ¹⁹K. H. Becker, W. Groth, and D. Kley, *Z. Naturforsch. A* **20**, 748 (1965).
- ²⁰R. C. M. Learner, *Proc. R. Soc. London Ser. A* **269**, 311 (1962).
- ²¹R. A. Sutherland and R. A. Anderson, *J. Chem. Phys.* **58**, 1226 (1973).
- ²²A. C. Vikis, *J. Chem. Phys.* **69**, 4314 (1978).
- ²³A. Fontijn, C. B. Meyer, and H. I. Schiff, *J. Chem. Phys.* **40**, 64 (1964).
- ²⁴*JANAF Thermochemical Tables*, 2nd ed., D. R. Stull and H. Prophet, Project Directors, Natl. Stand. Ref. Data Ser., Nat. Bur. Stand. (U.S.), **37**, 1971.
- ²⁵M. Lenzi and H. Okabe (unpublished results).
- ²⁶K. E. Holdy, L. C. Klotz, and K. R. Wilson, *J. Chem. Phys.* **52**, 4588 (1970).
- ²⁷G. E. Busch and K. R. Wilson, *J. Chem. Phys.* **56**, 3626 (1972).

- ²⁸L. Wallace, *Astrophys. J. Suppl.* **7**, 165 (1962).
- ²⁹D. D. Davis and H. Okabe, *J. Chem. Phys.* **49**, 5526 (1968).
- ³⁰J. W. C. Johns, *Can. J. Phys.* **41**, 209 (1962);
- ³¹M. Schürgers and K. H. Welge, *Z. Naturforsch. A* **23**, 1508 (1968).
- ³²M. N. R. Ashfold and J. P. Simons, *J. Chem. Soc. Faraday Trans. II* **74**, 208 (1978).
- ³³M. Savety-Dzvonick and R. Cody, *J. Chem. Phys.* **64**, 4794 (1976).
- ³⁴K. J. Miller, S. R. Mielczarek, and M. Krauss, *J. Chem. Phys.* **51**, 26 (1969).
- ³⁵F. Flouquet and J. A. Horsley, *J. Chem. Phys.* **60**, 3767 (1974).
- ³⁶M. N. R. Ashfold, M. T. MacPherson, and J. P. Simons, *Chem. Phys. Lett.* **55**, 84 (1978).
- ³⁷M. N. R. Ashfold and J. P. Simons, *J. Chem. Soc. Faraday Trans. II* **73**, 858 (1977).
- ³⁸R. J. Cody and M. J. Sabety-Dzvonik, and W. M. Jackson, *J. Chem. Phys.* **66**, 2145 (1977).
- ³⁹K. H. Welge and F. Stuhl, *J. Chem. Phys.* **46**, 2440 (1967).
- ⁴⁰M. N. R. Ashfold and J. P. Simons, *J. Chem. Soc. Faraday Trans. II* **74**, 1263 (1978).
- ⁴¹A. P. Cox and J. M. Riveros, *J. Chem. Phys.* **42**, 3106 (1965).